

On the Mechanism of Ligand-Assisted, Copper-Catalyzed Benzylic Amination by Chloramine-T

Dipti N. Barman,[†] Peng Liu,[‡] Kendall N. Houk,[‡] and Kenneth M. Nicholas^{*,†}

[†]Department of Chemistry and Biochemistry, University of Oklahoma, Norman, Oklahoma 73019, and

[‡]Department of Chemistry and Biochemistry, University of California, Los Angeles, California 90095

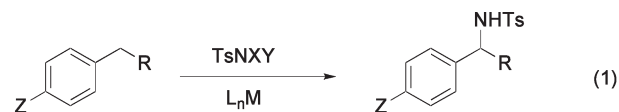
Received May 5, 2010

The mechanism of hydrocarbon amination by chloramine-T derivatives catalyzed by (diimine)-copper complexes has been investigated. The initial synthetic study of the reactions revealed ligand-accelerated catalysis, significant sensitivity to the electronic character of the substrates, and low to moderate enantioselectivities with homochiral ligands. Various mechanistic probes, both experimental and computational, have been focused on the C–H insertion process. A kinetic isotope effect of 4.6 was found in the amination of α -D(H)-cumenes catalyzed by [(diimine)Cu(solvent)]Z. Amination of the isomeric substrates *cis*- and *trans*-4-*tert*-butyl-1-phenylcyclohexanes with 4-Me-C₆H₄SO₂-NNaCl (chloramine-T) or 4-NO₂-C₆H₄SO₂NNaCl (chloramine-N) catalyzed by [(diimine)Cu(CH₃CN)]PF₆ produced in all cases an approximately 1:1 mixture of the corresponding *cis*- and *trans*-4-*tert*-butyl-1-phenyl-1-sulfonaminocyclohexanes. Amination of the radical-clock substrate 1-phenyl-2-benzylcyclopropane with chloramine-T/(diimine)Cu(CH₃CN)]PF₆ gave a mixture of ring-opened and cyclopropylmethylamino derivatives. Together, these results are most consistent with a stepwise insertion of an N-Ts(Ns) unit into the C–H bond, via carbon radicals, and a secondary contribution from a concerted insertion pathway. B3LYP and CASSCF computations suggest that the C–H insertion step involves the reaction of the hydrocarbon with a Cu-imido (nitrene) complex, [(diimine)-Cu=NSO₂R]⁺. The ground-state triplet of the Cu-imido complex is calculated to be 3–13 kcal/mol more stable than the singlet complex, depending on the method and basis sets employed. The reaction of each complex with toluene is modeled to find that the C–H insertion transition state for the triplet ($\Delta G^\ddagger = 8.2$ kcal/mol) is lower in energy than the singlet. The former reacts by a stepwise H-atom abstraction, while the latter reacts by a concerted C–H insertion. These results and kinetic isotope effect calculations for the singlet (2.9) and triplet (4.8) pathways, respectively, agree with the experimental observations (4.6) and point to a major role for the triplet complex in the stepwise, nonstereoselective insertion pathway.

Introduction

Amines and their derivatives constitute the most important class of synthetic and natural bioactive compounds, and they find numerous important uses in medicine and agriculture and as materials, dyes, and electronics. The importance and ubiquity of the amino functionality has motivated chemists

to develop new nitrogenation methods involving nitrenoid transfer reactions, either via addition to C–C unsaturation, i.e., aziridination,¹ or by insertion into the C–H bonds of hydrocarbons (eq 1).² Complexes of many transition metals have been found to catalyze such reactions using several N-reagents, most commonly imidiodinanes (ArI=NX), azides (Z–N₃), or haloamine derivatives (ZNNaX).



The chemo-, regio-, and stereoselectivities of these emerging nitrogenation processes are of paramount synthetic importance. Several systems studied to date effect aziridinations with moderate to excellent enantioselectivities employing chiral metal complex catalysts.³ Interestingly, some of these same reagent/catalyst systems do not react stereospecifically; for example,

*To whom correspondence should be addressed. E-mail: knicholas@ou.edu.

(1) (a) Evans, D. A.; Faul, M. M.; Bilodeau, M. T.; Anderson, B. A.; Barnes, D. M. *J. Am. Chem. Soc.* **1993**, 115, 5328. (b) Mueller, P.; Fruit, C. *Chem. Rev.* **2003**, 103, 2905. (c) Liang, J.-L.; Huang, J.-S.; Yu, X.-Q.; Zhu, N.; Che, C.-M. *Chem.—Eur. J.* **2002**, 8, 1563. (d) Li, Z.; Quan, R. W.; Jacobsen, E. N. *J. Am. Chem. Soc.* **1995**, 117, 5889. (e) Mairena, M. A.; Diaz-Requejo, M. M.; Belderrain, T. R.; Nicasio, M. C.; Trofimenko, S.; Perez, P. *J. Organometallics* **2004**, 23, 233.

(2) (a) Li, Z.; Capretto, D. A.; Rahaman, R.; He, C. *Angew. Chem., Int. Ed.* **2007**, 46, 5184. (b) Thu, H.-Y.; Yu, W.-Y.; Che, C.-M. *J. Am. Chem. Soc.* **2006**, 128, 9048. (c) Reed, S. A.; Mazzotti, A. R.; White, M. C. *J. Am. Chem. Soc.* **2009**, 131, 11701. (d) Wang, Z.; Zhang, Y.; Fu, H.; Jiang, Y.; Zhao, Y. *Org. Lett.* **2008**, 10, 1863. (e) Collet, F.; Dodd, R. H.; Dauban, P. *Chem. Commun.* **2009**, 5061–5074. (f) Davies, H. M. L.; Long, M. S. *Angew. Chem., Int. Ed.* **2005**, 44, 3518–3520. (g) Kalita, B.; Lamar, A. A.; Nicholas, K. M. *Chem. Commun.* **2008**, 4291.

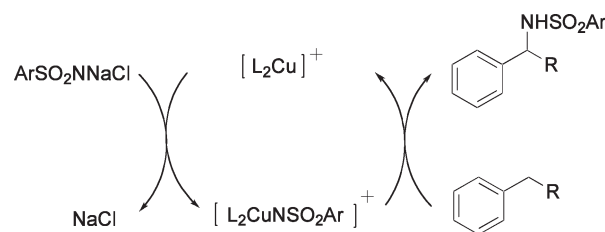
(3) Gillespie, K. M.; Sanders, C. J.; O'Shaughnessy, P.; Westmoreland, I.; Thickett, C. P.; Scott, P. *J. Org. Chem.* **2002**, 67, 3450–3458.

cis-olefins, unless constrained within a ring, often produce *cis/trans* aziridine product mixtures,⁴ suggestive of a stepwise formation of the two C–N bonds. The stereoselectivity of C–H aminations has not been investigated extensively, but *intramolecular* L_2Rh_2 -⁵ and $Ru(pybox^*)$ -catalyzed reactions, reagent-based $[ArS^*(O)(NSO_2Ar)NH_2]/Rh$ -catalyzed *intermolecular* reactions,⁷ and (salen)Mn-catalyzed *intermolecular* aminations of benzylic substrates⁸ have been reported with moderate to high enantioselectivities, consistent with a concerted C–H insertion process.

These selectivity features are determined primarily by the nature of the reactive N-species that is involved in the step(s) in which the C–N bond(s) is(are) formed. For the most part the reactive intermediates in metal-catalyzed aziridinations and C–H aminations are unknown. It has been generally assumed, with some supporting evidence, that metal-imido (nitrene) complexes, $LM=NZ$, are the active N-transfer agents, rather than free nitrenes. Only in a few instances have structurally characterized imido complexes been isolated and shown to effect aziridination or C–H insertions. Che and co-workers have investigated the reactions of isolable (porphyrin) $Ru(NSO_2R)_2$ complexes, which both aziridinate olefins and aminate hydrocarbon C–H bonds.⁹ Kinetics and redox potentials have been interpreted in terms of stepwise radical pathways with both classes of substrates. Recently, Warren and co-workers reported on the C–H insertion reactivity of dinuclear [(ketoiminato)Cu–N(adamantyl)]₂.¹⁰ Kinetic isotope effects, correlations with C–H bond dissociation energies, and DFT computational studies by the Cundari group¹¹ suggest that a monometallic $LCu(NR)$ singlet diradical species is responsible for the C–H insertion.

Aside from the systems involving isolable metal-imido complexes, some insights have been gained from mechanistic probes of other metal-catalyzed aziridinations and aminations presumed to involve imido-metal intermediates. The C–H(D) kinetic isotope effects, Hammett studies, radical-clock probes, and high intramolecular stereoselectivities observed in the Rh_2X_4 -catalyzed C–H aminations point to the intervention of an electrophilic imido- Rh_2 complex, which effects concerted C–H insertion.¹² Among the mechanistic studies of copper-catalyzed aziridination, the general picture is less clear. Some Cu-catalyzed aziridinations employing suitable chiral ligands achieve high enantioselectivities,¹³ although olefin stereochemistry is not always retained as expected for a concerted process. Kinetic analysis, Hammett substituent

Scheme 1



studies, and the common stereoselectivity found independent of the aminating agent have been interpreted in terms of the intervention of an electrophilic $LCu=NZ^{(+)}$ as the active nitrogenating species.¹⁴ Computational studies of various imido-Cu complexes with different N-donor auxiliary ligands have mostly supported a ground-state triplet state for such species¹⁵ (the Warren/Cundari system notwithstanding¹¹), which reacts stepwise as a N-centered radical with substrate-dependent competing C–C rotation versus C–N ring closure.

As part of an ongoing project to discover and elucidate new metal-catalyzed nitrogenation reactions of hydrocarbons, we recently have focused on the amination of benzylic substrates. An efficient system for benzylic amination was first developed employing readily available anhydrous chloramine-T ($MeC_6H_4SO_2NNAr$) with commercial $[Cu(CH_3CN)_4]PF_6$ (**1**) as catalyst.¹⁶ We then sought to identify suitable ligand partners for copper that could provide tailored catalytic activity and selectivity. Several ligand types, including phosphines, amines, α -amino acids, and diimines (Schiff bases), were indeed found to enhance catalytic amination activity (ligand-accelerated catalysis)¹⁷ relative to weakly ligated **1**.¹⁸ Within a series of *para*-substituted aryl-diimine ligands and aryl-substituted hydrocarbons the catalytic activity was found to increase with more electron-deficient ligands and more electron-rich substrates, indicative of an electrophilic aminating species, possibly $[L_2CuNSO_2Ar]^+$ (Scheme 1). A survey of the amination of prochiral benzylic substrates by chloramine-T catalyzed by complexes of *homochiral* amino acids and diimines, however, achieved only low to modest enantioselectivities (0–35%). These results caused us to consider further the identity of the aminating species in these reactions and the origin of its limited enantioselectivity. To address these issues, we have conducted a mechanistic study, including both experimental and computational probes, focusing on the crucial C–H insertion process. The results of this investigation are reported herein.

Results and Discussion

Experimental Studies. The primary focus of our experimental mechanistic investigation is the C–H/C–N substitution process itself. The key questions are, (1) is the substitution

(4) Caine, D.; O'Brien, P.; Rosser, C. M. *Org. Lett.* **2002**, *4*, 1923–1926.

(5) (a) Fleming, J. J.; Fiori, K. W.; Du Bois, J. J. *Am. Chem. Soc.* **2003**, *125*, 2028. (b) Fiori, K. W.; Fleming, J. J.; Du Bois, J. *Angew. Chem., Int. Ed.* **2004**, *43*, 4349.

(6) Milczek, E.; Boudet, N.; Blakey, S. *Angew. Chem., Int. Ed.* **2008**, *47*, 6825–6828.

(7) Shou, W. G.; Li, J.; Guo, T.; Lin, Z.; Jia, G. *Organometallics* **2009**, *28*, 6847–6854.

(8) Ohta, C.; Katsuki, T. *Tetrahedron Lett.* **2001**, *42*, 3885.

(9) (a) Leung, S. K.-Y.; Huang, J.-S.; Liang, J.-L.; Che, C.-M.; Zhou, Z.-Y. *Angew. Chem., Int. Ed.* **2003**, *42*, 340. (b) Liang, J.-L.; Yuan, S.-X.; Chan, P. W. H.; Che, C.-M. *Org. Lett.* **2002**, *4*, 4507. (c) Liang, J.-L.; Huang, J.-S.; Yu, X.-Q.; Zhu, N.; Che, C.-M. *Chem.—Eur. J.* **2002**, *8*, 1563. (d) Liang, J.-L.; Yuan, S.-X.; Huang, J.-S.; Yu, W.-Y.; Che, C.-M. *Angew. Chem., Int. Ed.* **2002**, *41*, 3465.

(10) Badiei, Y. M.; Krishnaswamy, A.; Melzer, M. M.; Warren, T. H. *J. Am. Chem. Soc.* **2006**, *128*, 15056.

(11) Badiei, Y. M.; Dinescu, A.; Dai, X.; Palomino, R. M.; Heinemann, F. W.; Cundari, T. R.; Warren, T. H. *Angew. Chem., Int. Ed.* **2008**, *47*, 9961.

(12) Fiori, K. W.; Espino, C. G.; Brodsky, B. H.; Du Bois, J. *Tetrahedron* **2009**, *65*, 3042.

(13) Müller, P.; Fruit, C. *Chem. Rev.* **2003**, *103*, 2905–2920.

(14) Li, Z.; Conser, K. R.; Jacobsen, E. N. *J. Am. Chem. Soc.* **1993**, *115*, 5326.

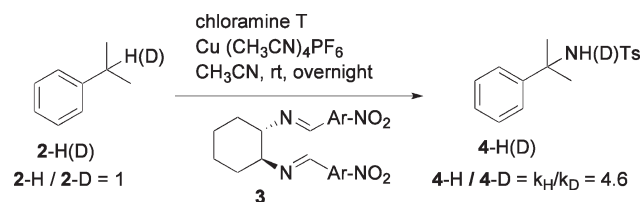
(15) (a) Brandt, P.; Soldergren, M. J.; Andersson, P. G.; Norrby, P. O. *J. Am. Chem. Soc.* **2000**, *122*, 8013–8020. (b) Conradie, J.; Ghosh, A. *J. Chem. Theory Comput.* **2007**, *3*, 689. (c) Meng, Q.; Wang, F.; Qu, X.; Zhou, J.; Li, M. *THEOCHEM* **2007**, *815*, 111. (d) Comba, P.; Lang, C.; Lopez de Laorden, C.; Muruganatham, A.; Rajaraman, G.; Wadepohl, H.; Zajączkowski, M. *Chem.—Eur. J.* **2008**, *14*, 5313. (e) Cundari, T. R.; Dinescu, A.; Kazi, A. B. *Inorg. Chem.* **2008**, *47*, 10067.

(16) Bhuyan, R.; Nicholas, K. M. *Org. Lett.* **2007**, *9*, 3957.

(17) Jacobsen, E. N.; Markó, I. E.; Mungall, W. S.; Schröder, G. W.; Sharpless, K. B. *J. Am. Chem. Soc.* **1988**, *110*, 1968.

(18) Barman, D. N.; Nicholas, K. M. *Tetrahedron Lett.* **2010**, *51*, 1815.

Scheme 2



reaction rate-limiting? (2) is the process concerted or stepwise? (3) is it stereoselective and, if so, in what sense, i.e., retention/inversion? and (4) what is the active aminating agent?

Our preliminary substrate and ligand-based reactivity survey (*op. cit.*) showed significant electronic effects, suggesting that the C–H insertion step could be rate-limiting. To address this issue further, we carried out a competitive amination reaction between cumene and α -d₁-cumene to determine the kinetic isotope effect (Scheme 2). A 1:1 mixture of the isotopomers **2-H(D)** was added to the preformed complex from diimine **3** and $[\text{Cu}(\text{CH}_3\text{CN})_4]\text{PF}_6$ in CH_3CN (20 °C), followed by addition of anhydrous chloramine-T. After a minimal workup to avoid H/D exchange GC-MS analysis of the reaction mixture found the ratio of sulfonamides **4-H/4-D** and the isotope effect to be 4.6 at 40% conversion; analysis of the unreacted cumene gave a kinetic isotope effect (KIE) of 3.5. This sizable primary KIE indicates that C–H bond-breaking is at least partially rate-limiting.

To further probe the nature of the C–H insertion step, especially its concertedness, we examined the stereoselectivity of the Cu-catalyzed amination with a pair of diastereomeric hydrocarbon substrates, *cis*- and *trans*-1-*tert*-butyl-4-phenylcyclohexane (**5-C**, **5-T**). A concerted insertion pathway is expected to be stereospecific; that is, the respective isomeric substrates should produce opposite isomeric products with high selectivity. Each substrate was separately treated with chloramine-T in the presence of the preformed catalyst from biphenyldiimine ligand **7** and $[\text{Cu}(\text{CH}_3\text{CN})_4]\text{PF}_6$ under typical conditions (Scheme 3).¹⁷ Chromatographic purification of the mixture from the reaction with *cis*-1-*tert*-butyl-4-phenylcyclohexane (**5-C**) provided an inseparable mixture of the isomeric 1-*tert*-butyl-4-phenyl-tosylamide-cyclohexanes (**8-C/8-T**, 33% yield) in a 1:1 ratio. *trans*-1-*tert*-Butyl-4-phenylcyclohexane (**5-T**) was similarly aminated to give a nearly identical isomeric mixture of amination products **8-C/8-T** in 28% combined yield. These results strongly suggest the primary operation of a nonconcerted process for the C–H insertion, likely proceeding through a common intermediate.

We wondered whether the electronic character of the aminating species could be sufficiently altered to affect the concertedness of the insertion step and hence its stereoselectivity. To test this idea, the nosylation of *trans*-1-*tert*-butyl-4-phenylcyclohexane (**5-T**) was examined using 4-O₂N-C₆H₄-SO₂NNaCl (**6b**), “chloramine-N” (Scheme 3). In this case a separable mixture of isomeric 4-*tert*-butyl-1-phenyl-1-nosylcyclohexanes (**9-C/9-T**) was obtained (38% combined yield), still in a nearly 1:1 ratio. Clearly, the nosylamino transfer agent still effects C–H insertion primarily by a stepwise, nonstereoselective process.

The nonstereoselective feature of the C–H/N substitution suggested the possibility of a stereorandomizing carbon radical or carbocation intermediate. To test the validity of this hypothesis, we chose the benzylic cyclopropyl substrate **10** for amination, anticipating that if either a radical or a

cation was generated at C-1, ring-opened amination products, e.g., *N*-(1,4-diphenylbut-3-enyl)-4-methylbenzene-sulfonamide (**12**), would be produced via rapid ring-opening (ca. $2 \times 10^9 \text{ s}^{-1}$) of the intermediate.¹⁹ Amination of *trans*-**10** under the standard conditions with chloramine-T catalyzed by $[(\text{3})\text{Cu}(\text{CH}_3\text{CN})]\text{PF}_6$ produced a mixture of cyclic sulfonamide **11** (6%) and ring-opened products **12-C/12-T** (18%). Hence we conclude that the nitrenoid C–H insertion occurs stepwise and proceeds via H-atom (or hydride) abstraction to form the C-1 radical (or cation). Although the formation of ring-opened products cannot unambiguously differentiate radical from carbocation intermediates, the relatively modest substrate substituent effects that were observed in our synthetic studies²⁰ and the computational modeling (*vide infra*) favor the intervention of radicals.

Computational Studies. To understand the mechanism and concertedness of the Cu-catalyzed amination reactions of chloramine-T, we have performed DFT and CASSCF calculations on both singlet and triplet pathways of this reaction. We focused on the C–H insertion reaction of the Cu-imido complex since this process is stereoselectivity-determining and, based on the KIE results, at least partially rate-limiting.

The mechanisms of a related reaction thought to involve Cu-imido intermediates, Cu-catalyzed alkene aziridinations with $\text{PhI}=\text{NTs}$ and TsN_3 , have been investigated previously by both experiment and theory. Kinetic and theoretical studies by Jacobson,^{1d} Norrby,^{15a} and Comba^{15d} suggest that the aziridination reactions occur via a Cu(I)/Cu(III) cycle involving a Cu-imido complex $\text{LCu}=\text{NTs}$ as the reactive intermediate. DFT calculations also suggest that Cu(II) precatalysts can enter the catalytic cycle through reduction by $\text{PhI}=\text{NTs}$ to Cu(I). On the other hand, alternative mechanisms involving Cu(II) active species were proposed by Pérez²¹ and Vedernikov.²²

Due to their high reactivities, no terminal imido-copper complexes have been structurally characterized. However, their structure and spin state have been investigated using several levels of theory. Density functional theory calculations suggest a ground triplet state for cationic LCu-imido complexes.¹⁵ However, recent CASSCF^{11,15e} and ccCA²³ (correlation consistent composite approach) calculations by Cundari and co-workers suggest that a biradical singlet is the ground state for neutral (β -diketiminate)Cu(NPh) and (β -diketiminate)Cu(NH) complexes. A recent DFT study on Ni-nitrene complexes by the Cundari group suggested that the singlet–triplet gap is affected by the nitrene substituent. The singlet ground states are favored when aryl/alkyl groups are on the nitrene,²⁴ while the triplet is favored with electron-withdrawing heteroatom groups (like $-\text{SO}_2\text{R}$).²⁵

In this study, we investigated the structures and spin state of Cu-imido complexes and the C–H insertion transition

(19) Davis, A. F.; Song, M. M.; Alexander, A. *J. Org. Chem.* **2006**, *71*, 2779.

(20) Johnson, C. C.; Lippard, S. J.; Liu, K. E.; Newcomb, M. *J. Am. Chem. Soc.* **1993**, *115*, 939.

(21) Díaz-Requejo, M. M.; Pérez, P. J.; Brookhart, M.; Templeton, J. L. *Organometallics* **1997**, *16*, 4399.

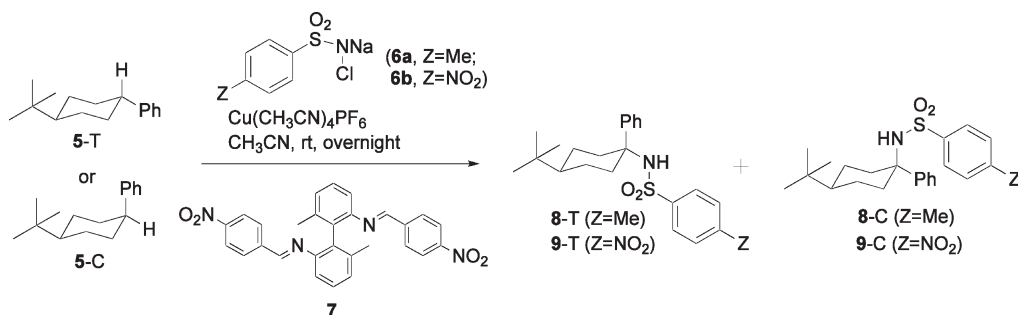
(22) Mohr, F.; Binfield, S. A.; Fetting, J. C.; Vedernikov, A. N. *J. Org. Chem.* **2005**, *70*, 4833.

(23) Tekarli, S. M.; Williams, T. G.; Cundari, T. R. *J. Chem. Theory Comput.* **2009**, *5*, 2959.

(24) (a) Cundari, T. R.; Vaddadi, S. *THEOCHEM* **2006**, *801*, 47. (b) Cundari, T. R.; Pierpont, A. W.; Vaddadi, S. *J. Organomet. Chem.* **2007**, *692*, 4551. (c) Cundari, T. R.; Jimenez-Halla, J. O. C.; Morello, G. R.; Vaddadi, S. *J. Am. Chem. Soc.* **2008**, *130*, 13051.

(25) Cundari, T. R.; Morello, G. R. *J. Org. Chem.* **2009**, *74*, 5711.

Scheme 3



Scheme 4

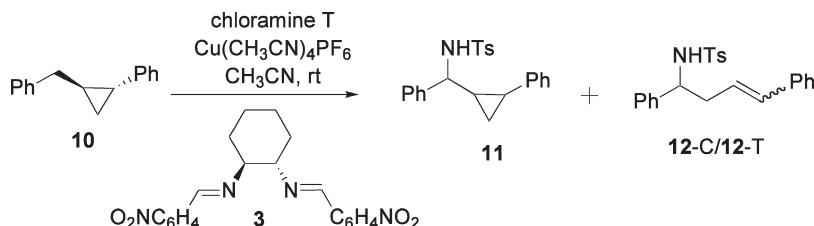


Table 1. Singlet/Triplet Splitting of the [(diimine)Cu=NSO₂Me]⁺ Complex 13 by Various Levels of Calculations

method	ΔE (kcal/mol) ^a	ΔG (kcal/mol) ^a
B3LYP/LANL2DZ-6-31G(d)	-3.3	-5.8
B3LYP/SDD-6-311 + G(d)	-1.8	-4.3
B3LYP/6-311 + G(d)	-0.2	-2.8
CASSCF(10,10)/CEP-31G(d)//B3LYP/LANL2DZ-6-31G(d)	-10.1	-12.6 ^b
CASSCF(12,12)/CEP-31G(d)//B3LYP/LANL2DZ-6-31G(d)	-10.7	-13.2 ^b
CASSCF(10,10)/CEP-31G(d)	-7.5	-7.5 ^b
CASSCF(10,10)/LANL2DZ	-11.6	-11.1 ^b

^a Electronic energies and Gibbs free energies are in kcal/mol, defined as $E(\text{triplet}) - E(\text{singlet})$. Negative number means triplet ground state.

^b Thermal and entropic corrections are calculated at the B3LYP/LANL2DZ-6-31G(d) level.

state at several theoretical levels. *N,N'*-Dimethylene-1,2-ethylenediamine was used as a model ligand. Calculations using a real ligand that has been used experimentally suggest the singlet/triplet splitting is similar to the model system (see Supporting Information for details). *N*-SO₂Me was used as a surrogate for the *N*-SO₂Tol in the calculations.

We first calculated the singlet/triplet splitting of [(diimine)Cu=NSO₂Me]⁺ **13** using B3LYP and CASSCF with several basis sets. The results are shown in Table 1. Both the B3LYP and CASSCF calculations suggest a triplet ground state for the Cu-imido complex, although the singlet/triplet splitting varies from -2.8 to -13.2 kcal/mol by different methods. B3LYP calculations with a mixed basis set of LANL2DZ effective core potential basis set for Cu and 6-31G(d) for other atoms predict that the triplet complex is 5.8 kcal/mol more stable than the singlet complex. Using a smaller-core pseudopotential SDD for Cu and 6-311 + G(d) for other atoms, a slightly smaller S/T splitting of -4.3 kcal/mol was predicted. The full-electron basis set 6-311 + G(d) on all atoms including Cu predicts an even smaller splitting of -2.8 kcal/mol. This agrees with the previous B3LYP study by Norrby and co-workers, whose calculations with a full-electron basis set predict small singlet/triplet splitting, while effective core potential basis sets predict a much more stable

triplet ground state.^{15a} Single-point CASSCF calculations on B3LYP/LANL2DZ-6-31G(d) geometries using a 10-electron-10-orbital active space and a 12-electron-12-orbital active space predicted very similar singlet/triplet splitting, suggesting a (10,10) active space is adequate for CASSCF calculations.²⁶ CASSCF geometry optimizations using CEP-31G(d) and LANL2DZ basis sets predict the triplet is 7.5 and 11.1 kcal/mol more stable than the singlet, respectively. This is in contrast to the CASSCF study by Cundari and co-workers on the (β -diketiminato)Cu-nitrene complexes, which predicts a singlet ground state. Since the Cu-N covalent bond order is greater²⁷ and thus more polarized in the singlet complex, Cu is more positively charged in the singlet complex than in the triplet. The Mulliken charges on the Cu of the singlet and the triplet complexes are 0.600 and 0.554, respectively. Electron-rich ligands such as β -diketiminato may stabilize the positive charge on the Cu atom and thus stabilize the singlet. At a reviewer's suggestion the effects of the N-substituent and the denticity of the sulfonimido ligand on the singlet/triplet gap were also evaluated. B3LYP calculations on the singlet/triplet splitting of [(diimine)Cu=N-Ph]⁺ and the κ^1 isomer of [(diimine)Cu=NSO₂Me]⁺ found that both complexes have triplet ground states with larger S/T splittings than the [κ^2 -(diimine)Cu=NSO₂Me]⁺ complex **13**.²⁸ This suggests that the oxygen atom bound to the Cu in the [κ^2 -(diimine)Cu=NSO₂Me]⁺ complex stabilizes the singlet by donating electrons to the Cu which is more positively charged in the singlet complex.

The CASSCF frontier molecular orbitals of the singlet and triplet Cu-imido complexes are shown in Figure 1. The two singly occupied orbitals in the triplet complex are the in-plane Cu d_{xy} orbital and the out-of-plane p orbital of the imido N, respectively (Figure 1b). The spin density of the triplet complex is mainly located at the imido N (1.180) and

(26) Cundari et al. also used a (10,10) active space with the CEP-31G(d) basis set in their CASSCF study on Cu-nitrene complexes. See ref. 15e.

(27) NBO calculations predict that the Cu-N Wiberg bond indices are 0.454 and 0.771 for the triplet and singlet complex, respectively.

(28) See Supporting Information for more details about these calculations.

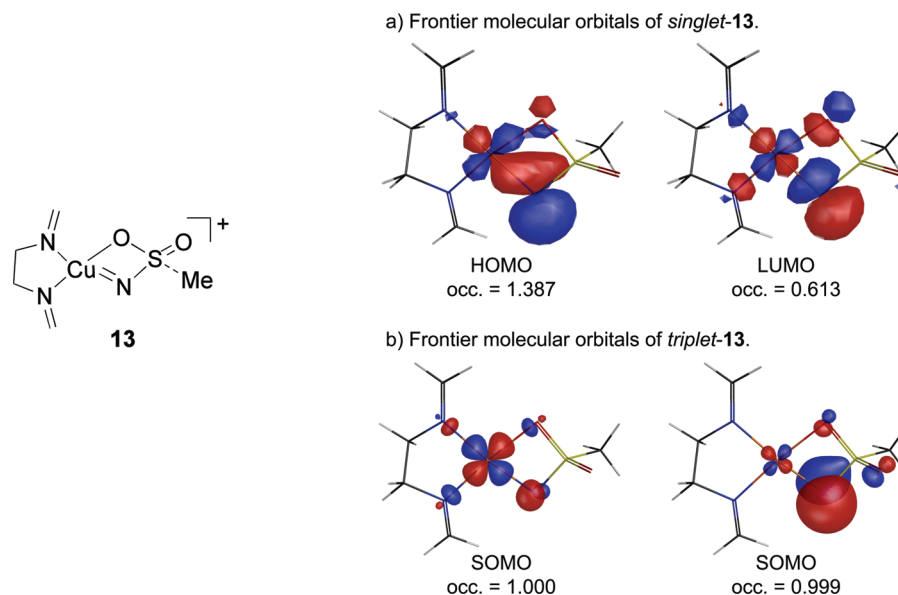


Figure 1. Frontier molecular orbitals of *singlet*- and *triplet-13* from CASSCF(10,10)/CEP-3G(d) calculations.

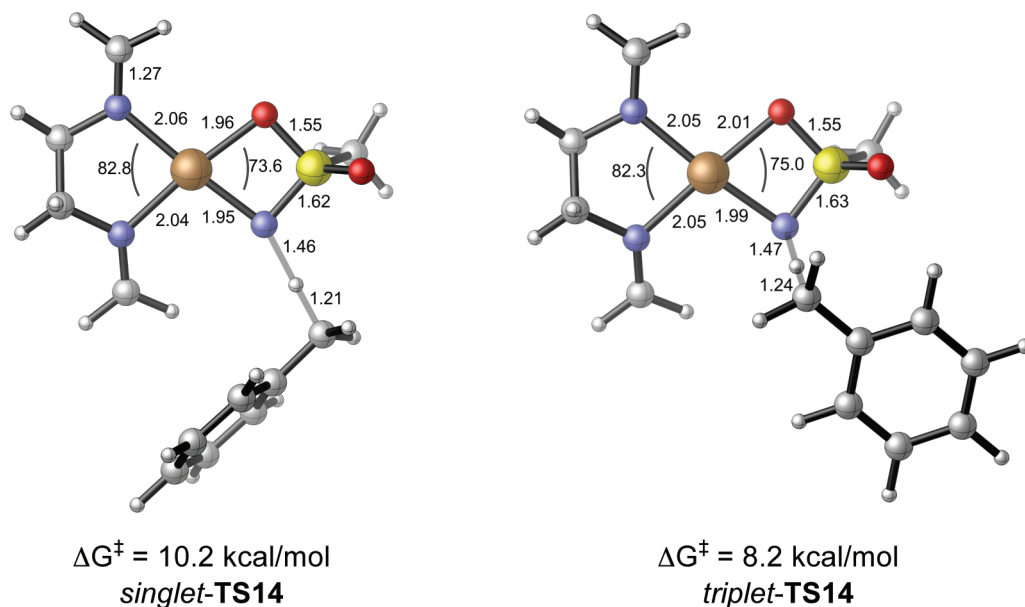


Figure 2. Transition-state structures of *singlet*- and *triplet-TS14* from B3LYP/LANL2DZ-6-31G(d) calculations.

Cu (0.437) atoms, in agreement with the FMO analysis. The Cu–imido-N bond length in the triplet complex is longer than in the singlet complex (2.00 and 1.87 Å, respectively, for B3LYP/LANL2DZ-6-31G(d)-optimized geometries; 2.04 and 1.96 Å, respectively, for CASSCF(10,10)/CEP-31G(d)-optimized geometries). These results suggest that the unpaired electrons of the triplet Cu-imido complex are mainly located on the imido N and Cu atoms and that subsequent C–H insertion is most likely to occur at the imido N atom.

The C–H insertion occurs via hydrogen atom transfer from the toluene to the amido nitrogen atom of the LCu-imido complex. In the triplet C–H insertion transition state *triplet-TS14* (Figure 2), the toluene hydrogen approaches the perpendicular position of the imido-N, since the radical character is mainly located at the out-of-plane p orbital of the nitrogen. The angle of the attack is 119° as predicted by B3LYP calculations and 141° by CASSCF calculations.

In contrast, in the singlet transition state, *singlet-TS14* (Figure 2), the toluene attacks the in-plane position of the Cu-imido complex. The HOMO and LUMO of the singlet Cu-imido complex involve the $\sigma_{\text{Cu-N}}$ bonding and the $\sigma_{\text{Cu-N}}^*$ antibonding orbitals, respectively; both are in the same plane of the Cu-imido complex (Figure 1a). B3LYP calculations predict the angle of the attack via the singlet pathway is 170°, and CASSCF predicts 165°.

The triplet C–H insertion transition state is 2.0 and 1.3 kcal/mol more stable than the singlet transition state, as predicted by B3LYP/LANL2DZ-6-31G(d) and CASSCF (10,10)/CEP-31G(d) calculations, respectively. IRC calculations on both singlet and triplet transition states were performed to determine the concertedness of both pathways. The IRC calculations on the singlet transition state *singlet-TS14* lead directly to the amination product and the Cu being bound to the oxygen atom in the product complex

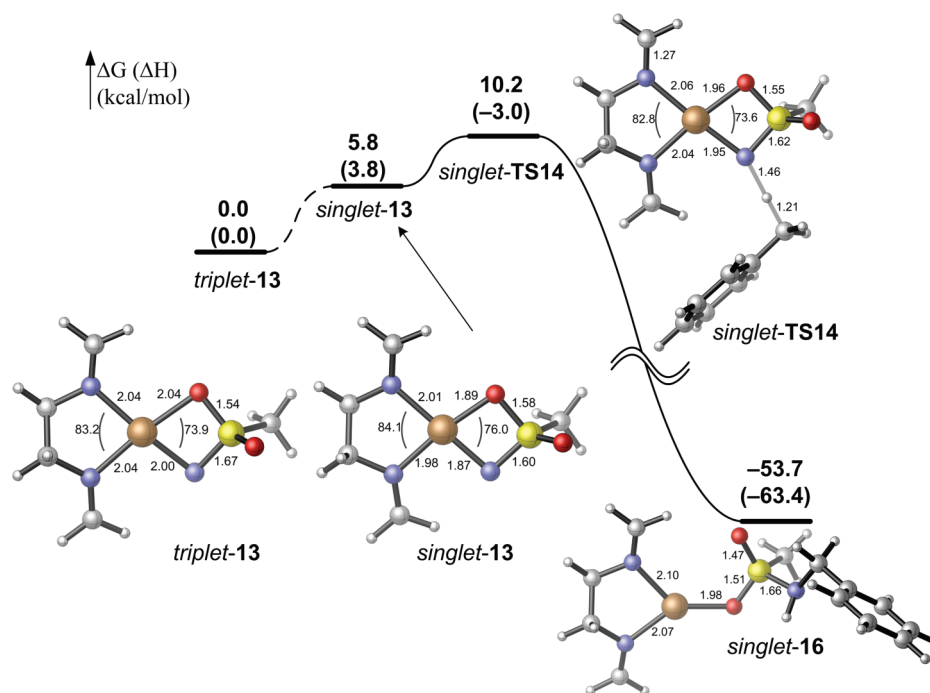


Figure 3. Potential energy profile for the singlet pathway at the B3LYP/LANL2DZ-6-31G(d) level.

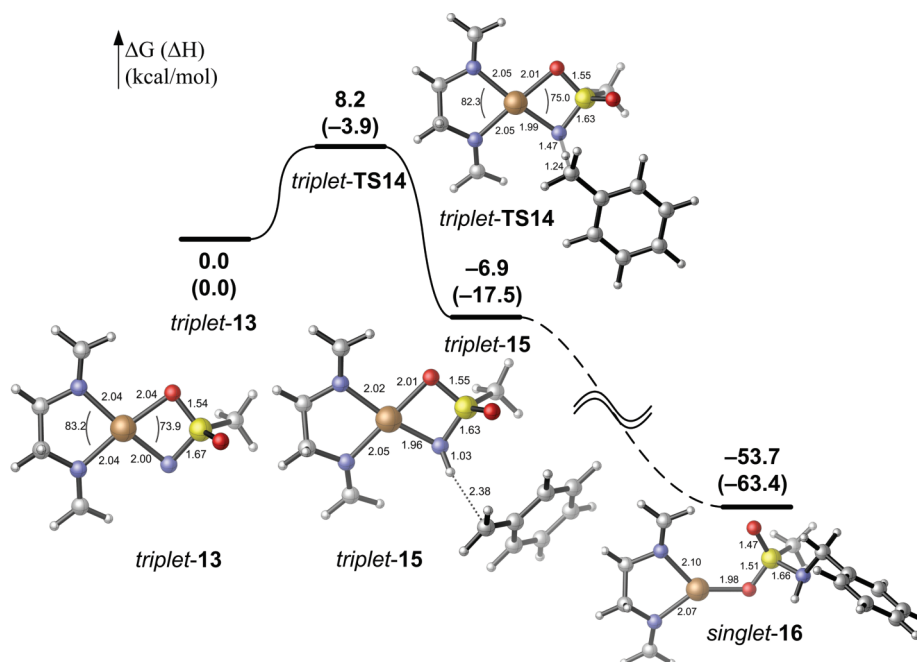


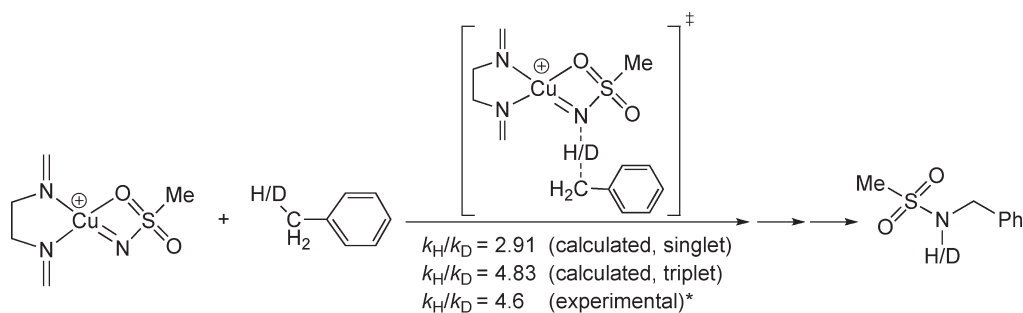
Figure 4. Potential energy profile for the triplet pathway at the B3LYP/LANL2DZ-6-31G(d) level.

singlet-16. In contrast, the triplet transition state *triplet-TS14* leads to a radical pair intermediate *triplet-15*, a weakly bound complex of benzyl and [LCu-NH-SO₂Me]⁺ radicals. The positive charge is mainly located on the Cu-imido complex, and the benzyl radical is almost neutral. This suggests the intermediate in the triplet C–H insertion is a carbon radical rather than a carbocation. Recombination of the radical pair may occur via multiple mechanisms: spin crossover to form a singlet radical pair followed by rapid radical combination or intermolecular radical coupling. In either case, carbon configuration may be lost during the

formation of the singlet LCu-product complex *singlet-16* from the radical pair intermediate *triplet-15*. The triplet LCu-product complex *triplet-16* is much less stable than the singlet.

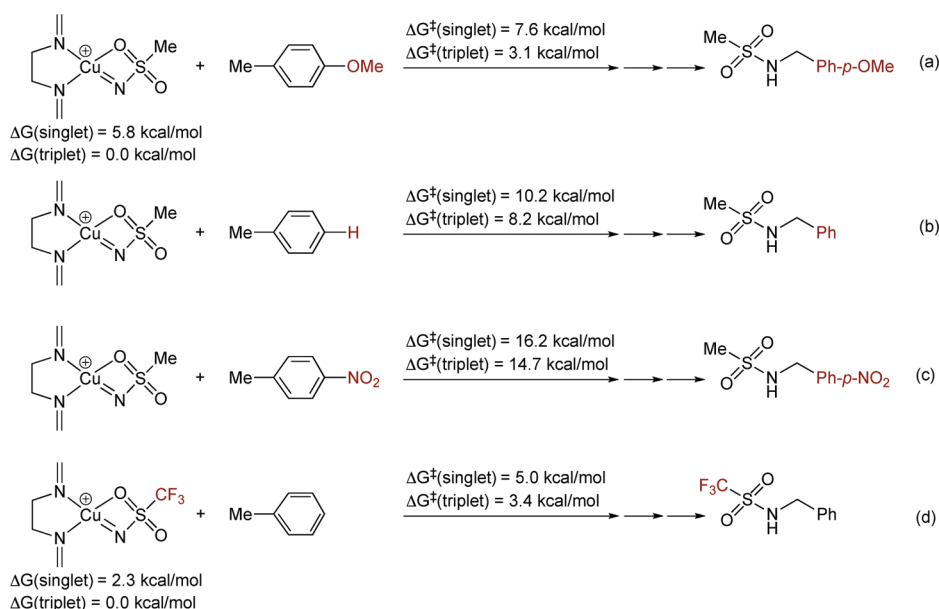
The Gibbs free energy and enthalpy profiles for C–H insertion of toluene via singlet and triplet pathways were calculated at the B3LYP/LANL2DZ-6-31G(d) level and are shown in Figures 3 and 4, respectively. Transition states and intermediates in both profiles are with respect to the most stable triplet LCu-imido complex *triplet-13*. Steps involving spin crossover or radical termination are marked with dashed lines.

Scheme 5. Calculated and Experimental Kinetic Isotope Effects

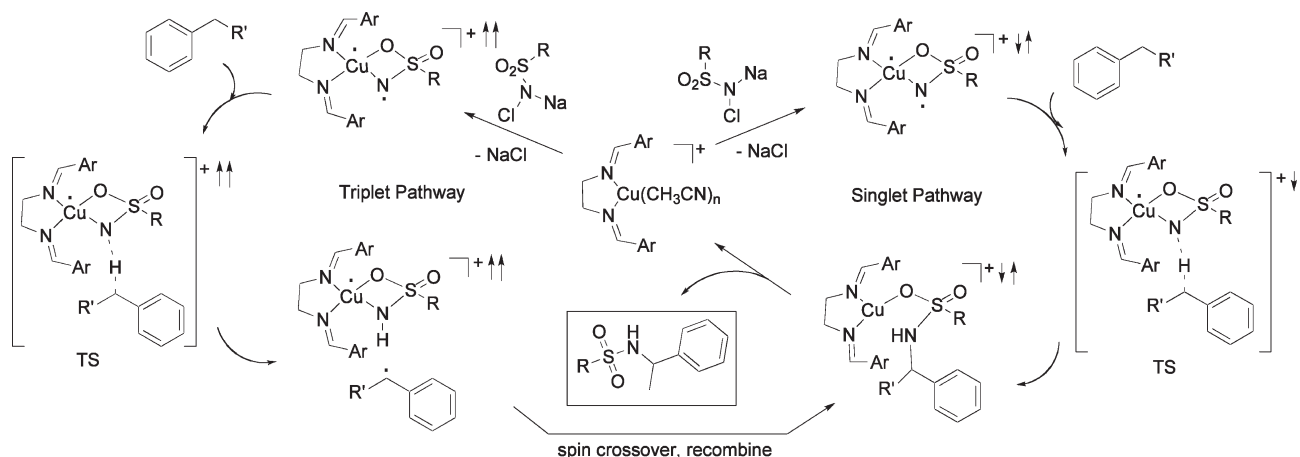


* different substrates and ligand were used in the experiment (see Scheme 2).

Scheme 6. C–H Activation Barriers at the B3LYP/LANL2DZ-6-31G(d)



Scheme 7. Mechanistic Pathways for (diimine)Cu-Catalyzed Amination by Chloramine-T



Kinetic isotope effects on the C–H insertion of toluene were calculated at the B3LYP/LANL2DZ-6-31G(d) level. The resulting KIEs for the singlet and triplet pathways are 2.91 and 4.83, respectively. The experimentally observed KIE for the reaction with toluene is 4.6 (Scheme 5), in agreement with the calculated KIE for the triplet pathway.

We have also investigated the activation barriers for C–H insertion of representative electron-rich and electron-poor toluene derivatives (Scheme 6 (a)–(c)). The triplet C–H insertion transition state is favored in all cases. The more electron-rich methylanisole requires a lower barrier in the C–H insertion relative to toluene, and nitrotoluene is found

to have the largest barrier. These results agree with the qualitative experimental dependence of the rate and amination efficiency on the substrate structure.¹⁸ This indicates that the Cu-imido complex **13** is electrophilic and that *triplet-13* is more electrophilic than *singlet-13* since the singlet/triplet splitting of the transition state is larger for electron-rich substrates.

To study the electronic effects of substituents on the sulfonamide reagent, activation energies of the C–H insertion with two Cu-imido complexes, LCu–N–SO₂CH₃, and LCu–N–SO₂CF₃, were calculated using B3LYP. The results are given in Scheme 6 (b) and (d). Both Cu-imido complexes have a triplet ground state. An electron-withdrawing group on the sulfonamide decreases the singlet/triplet gap of the Cu-imido complex from 5.8 kcal/mol for LCu–N–SO₂CH₃ to 2.3 kcal/mol for LCu–N–SO₂CF₃. Both complexes still prefer the triplet pathway in C–H insertion. The singlet/triplet gaps of the C–H insertion transition states are similar: 2.0 kcal/mol for LCu–N–SO₂CH₃ and 1.6 kcal/mol for LCu–N–SO₂CF₃. An electron-withdrawing group on the sulfonamide decreases the C–H insertion activation energies for both the singlet and triplet pathways. These results suggest that sulfonamides with electron-withdrawing groups are more reactive, while the C–H insertion via the triplet pathway is slightly more favorable.

On the basis of these experimental and computational studies, we propose the mechanistic pathways outlined in Scheme 7. Considering all the evidence, the triplet pathway likely dominates. However, the modest (but nonzero) enantioselectivities observed in reactions catalyzed by chiral diimine complexes¹⁸ and the significant amount of ring-retained product from the radical-clock substrate suggest that the singlet pathway contributes to a minor extent.

Conclusions

The combined experimental observations of low enantioselectivity, a substantial primary kinetic isotope effect, negligible diastereoselectivity, and the formation of ring-opened products with the cyclopropyl substrate together are indicative of the predominant operation of a stepwise (nonconcerted) C–H insertion process, most likely through the intermediacy of C-centered radicals. Computational results support this picture with the primary reactive N-species being the triplet (diimine) Cu(NZ) complex, which acts as an N-centered radical, stepwise abstracting a H-atom from the substrate followed by radical rebound to form the C–N bond. A minor pathway involving concerted, stereoselective insertion via the singlet complex requires a somewhat higher activation energy but may also contribute. A primary kinetic isotope effect was observed, and calculations suggest that the KIE corresponds to the triplet C–H insertion transition state.

Experimental Section

General Procedures. Acetonitrile was refluxed over and distilled from calcium hydride. Some of the hydrocarbon substrates were obtained commercially and distilled before use. Commercial chloramine-T trihydrate was dried in a drying pistol over refluxing toluene under vacuum (0.1 mm) for 4–5 h; no thermal instability or decomposition was noted in any samples dried in this way. Cu(CH₃CN)₄PF₆ was obtained commercially. NMR spectra were recorded on a Varian Mercury NMR spectrometer at 300 MHz for ¹H and 75 MHz for ¹³C NMR spectra. All chemical shifts (ppm) reported are relative to the NMR solvent peak. Electrospray (ESI) mass spectra were recorded on a Finnigan TSQ 700 mass spectro-

meter. GC-mass spectra (electron impact) were obtained on an Agilent benchtop HP6890/MSD5973. The following compounds were prepared by literature methods: diimine ligands **3** and **7**,¹⁸ *N*-chloro-*N*-sodio-4-nitrobenzenesulfonamide,²⁹ cyclohexane derivatives **5-C** and **5-T**,³⁰ and cyclopropyl substrate **10**.³¹

Preparation of d₁-Cumene. The procedure was modified from the previously reported preparation.³² Commercially available cumene (2.0 mL, 19 mmol) was mixed with 10 wt % of Pd–C and 8 mL of D₂O, and the reaction flask was fitted with two balloons full of hydrogen. The mixture was stirred at room temperature overnight and then filtered through filter paper to remove the Pd–C. The reaction mixture was partitioned between ethyl acetate and water, and the organic phase was dried over MgSO₄ and concentrated by rotary evaporation. The deuterium content of the recovered cumene was determined by ¹H NMR integration of the methyl groups to the tertiary hydrogen.

D-Isotope Effect Determination. Commercial Cu(CH₃CN)₄PF₆ (19 mg, 0.049 mmol), diimine **3** (19 mg, 0.049 mmol), and 5 mL of dry CH₃CN were added to a round-bottom flask containing dry molecular sieves (4 Å, ca. 200 mg) under argon. To the well-stirred suspension was added the 1:1 mixture of cumene and deuterated cumene (68 μL, 0.49 mmol). Anhydrous chloramine-T (89 mg, 0.39 mmol) was added after one hour, and the mixture was stirred at room temperature overnight. The mixture was filtered through Celite to remove the precipitated copper salts and then analyzed by gas chromatography/mass spectrometry (GC-MS). The ratio of the d₀-product to the d₁-product (**4-H/4-D**) was 4.6:1.0. GC-MS (EI) analysis of the unreacted cumene-H/D in two separate runs gave *k_H*/*k_D* values of 3.3 and 3.7 (av = 3.5).

Aminosulfonation of *cis*-1-*tert*-Butyl-4-phenylcyclohexane. Commercial Cu(CH₃CN)₄PF₆ (28 mg, 0.073 mmol), diimine **7** (35 mg, 0.073 mmol), and 5 mL of dry CH₃CN were added to a round-bottom flask containing dry molecular sieves (4 Å, ca. 250 mg) under argon. To the well-stirred suspension was added *cis*-1-*tert*-butyl-4-phenylcyclohexane¹⁹ (**5-C**, 0.16 g, 0.73 mmol). Anhydrous chloramine-T (0.25 g, 1.1 mmol) was added to the reaction vessel after 30 min and the mixture stirred at room temperature overnight. The mixture was then filtered through Celite powder to remove insoluble metal-containing materials, and the solvent was evaporated under reduced pressure. The crude residue was purified by preparative TLC (3:1 hexane/ethyl acetate). The ratio of the inseparable isomeric products **8-T** and **8-C** was determined by integration of the tertiary butyl group of each isomer (found 1.0:1.0). Combined yield: 9.3 mg (33%). ¹H NMR (CDCl₃, 300 MHz): δ 8.96 (s, 1H), 7.88 (d, 2H, *J* = 8.1), 7.33–7.25 (m, 14H), 7.13 (d, 2H, *J* = 8.1), 7.04 (d, 2H, *J* = 8.4), 5.57 (s, 1H), 2.56 (d, 2H, *J* = 12.9), 2.47 (s, 3H), 2.45 (s, 3H), 2.22 (d, 2H, *J* = 12), 1.93–1.62 (m, 8H), 1.3–1.09 (m, 6H), 0.95 (s, 9H), 0.90 (s, 9H). ¹³C NMR (CDCl₃, 75 MHz): δ 167.0, 163.4, 146.9, 146.2, 142.9, 141.9, 140.6, 139.9, 129.5, 129.2, 128.8, 128.5, 127.7, 126.7, 126.2, 125.3, 59.6, 59.9, 47.5, 47.3, 38.63, 36.1, 32.6, 27.7, 23.2, 23.0, 22.8, 22.2, 21.7, 21.6. ESI-MS: *m/z* 408.21 (M + Na) 449.21 (M + CH₃CN + Na).

Aminosulfonation of *trans*-1-*tert*-Butyl-4-phenylcyclohexane. Commercial Cu(CH₃CN)₄PF₆ (0.028 g, 0.073 mmol), diimine ligand **7** (35 mg, 0.073 mmol), and 5 mL of dry CH₃CN were added to a round-bottom flask with dry molecular sieves (4 Å, ca. 200 mg) under an argon atmosphere. *trans*-1-*tert*-Butyl-4-phenylcyclohexane (**5-T**, 0.158 g, 0.73 mmol) was then added to the mixture. Anhydrous chloramine-T (251 mg, 1.1 mmol) was added after 30 min, and the reaction mixture was stirred at room

(29) Heintzelman, R. W.; Swern, D. *Synthesis* **1976**, 11, 731.

(30) Garbisch, E. W., Jr.; Patterson, D. B. *J. Am. Chem. Soc.* **1963**, 85, 3228.

(31) Bumgardner, C. L.; Iwerks, H. *J. Am. Chem. Soc.* **1966**, 88, 5518.

(32) Kurita, T.; Hattori, K.; Seki, S.; Mizumoto, T.; Aoki, F.; Yamada, Y.; Ikawa, K.; Maegawa, T.; Monguchi, Y.; Sajiki, H. *Chem.—Eur. J.* **2008**, 14, 664.

temperature overnight. The mixture was then filtered through Celite powder, and the solvent was evaporated under reduced pressure. The crude residue was purified by preparative TLC (3:1 hexane/ethyl acetate). Combined yield of **8-C**/**8-T**: 8.0 mg, yield 28%, white solid. The ratio of the isomers was determined by integration of the tertiary butyl group of each (found 1.0:1.0). ^1H NMR (CDCl_3 , 300 MHz): δ 8.96 (s, 1H), 7.88 (d, 2H, J = 8.1), 7.33–7.25 (m, 14H), 7.13 (d, 2H, J = 8.1), 7.04 (d, 2H, J = 8.4), 5.57 (s, 1H), 2.56 (d, 2H, J = 12.9), 2.47 (s, 3H), 2.45 (s, 3H), 2.22 (d, 2H, J = 12), 1.93–1.62 (m, 8H), 1.3–1.09 (m, 6H), 0.95 (s, 9H), 0.90 (s, 9H). ^{13}C NMR (CDCl_3 , 75 MHz): δ 167.0, 163.4, 146.9, 146.2, 142.9, 141.9, 140.6, 139.9, 129.5, 129.2, 128.8, 128.5, 127.7, 126.7, 126.2, 125.3, 59.6, 59.9, 47.5, 47.3, 38.6, 36.1, 32.6, 27.7, 23.2, 23.0, 22.8, 22.2, 21.7, 21.6. ESI-MS: m/z 408.21 ($\text{M} + \text{Na}$), 449.21 ($\text{M} + \text{CH}_3\text{CN} + \text{Na}$).

Aminonosylation of *trans*-1-*tert*-Butyl-4-phenylcyclohexane. Commercial $\text{Cu}(\text{CH}_3\text{CN})_4\text{PF}_6$ (10 mg, 0.025 mmol), diimine **7** (13 mg, 0.025 mmol), and 5 mL of dry CH_3CN were added to a round-bottom flask containing dry molecular sieves (4 Å, ca. 200 mg) under argon. To the well-stirred suspension was added *trans*-1-*tert*-butyl-4-phenylcyclohexane (**5-T**, 55 mg, 0.25 mmol). Anhydrous *N*-chloro-*N*-sodio-4-nitrobenzenesulfonamide (**6b**, 80 mg, 0.31 mmol) was added into the reaction vessel after one hour, and the mixture was stirred at room temperature overnight. The mixture was then filtered through Celite to remove the precipitated copper salts, and the solvent was evaporated under reduced pressure. NMR analysis of the crude product showed a 1:1 ratio of isomers from integration of the *tert*-butyl protons. The isomers **9-C** and **9-T** were separated by preparative TLC (3:1 hexane/ethyl acetate) but not stereochemically assigned. R_f (isomer 1) = 0.38; yield 12 mg (12%), white solid, mp 207–208 °C. ^1H NMR (CDCl_3 , 300 MHz): δ 7.92(d, 2H, J = 8.7), 7.33 (d, 2H, J = 8.7), 7.11 (d, 2H, J = 8.4), 7.04–6.97 (m, 3H), 4.80 (s, 1H), 2.76 (d, 2H, J = 11.1), 1.75 (t, 2H, J = 12.9, J = 12.9), 1.58 (d, 2H, J = 13.2), 0.91–0.78 (m, 3H), 0.634 (s, 9H). ^{13}C NMR (CDCl_3 , 75 MHz): δ 147.7, 137.5, 135.2, 128.2, 128.1, 127.8, 127.6, 123.4, 60.9, 47.5, 38.3, 32.2, 27.3, 23.6. ESI-MS (m/z): 416.21 ($\text{M} + \text{Na}$). R_f (isomer 2) = 0.15; yield 10 mg (10%); mp > 220 °C. ^1H NMR (CDCl_3 , 300 MHz): δ 8.05 (d, 2H, J = 8.7), 7.34–7.24 (m, 10H), 5.63 (s, 1H), 2.39 (d, 2H, J = 12.9), 1.75–1.62 (m, 6H), 1.18–1.031 (m, 2H), 0.9 (s, 9H).

Aminonosylation of *cis*-1-*tert*-Butyl-4-phenylcyclohexane. The amination reaction of *cis*-1-*tert*-butyl-4-phenylcyclohexane (**5-C**) was carried out in the same way as with the *trans* isomer. NMR analysis of crude product showed a 1:1 ratio of isomers **9-C**/**9-T** from the integration of the *tert*-butyl proton peaks.

Amination of 1-Benzyl-2-phenylcyclopropane. Commercial $\text{Cu}(\text{CH}_3\text{CN})_4\text{PF}_6$ (9.0 mg, 0.024 mmol), diimine **7** (7.0 mg, 0.024 mmol), and 5 mL of dry CH_3CN were added to a round-bottom flask containing dry molecular sieves (4 Å, ca. 200 mg) under argon. To the well-stirred suspension was added 1-benzyl-2-phenylcyclopropane (**10**, 50 mg, 0.24 mmol). Anhydrous chloramine-T (94 mg, 0.36 mmol) was added to the reaction vessel after 30 min, and the mixture was stirred at room temperature overnight. The mixture was then filtered through Celite, and the solvent was evaporated under reduced pressure. The crude residue was purified by preparative TLC (3:1 hexane/ethyl acetate)

to afford the cyclopropylmethyl amine derivative **11**; yield 5 mg (6%), white solid. ^1H NMR (CDCl_3 , 300 MHz): δ 7.66 (d, 2H, J = 8.1), 7.26–7.17 (m, 5H), 7.12–6.96 (m, 5H), 6.57 (d, 2H, J = 7.2), 4.96 (d, 1H, J = 10.5), 4.87 (d, 1H, J = 3), 4.61 (dd, 1H, J = 4.5, J = 5.1), 3.23–3.17 (m, 1H), 2.38 (s, 3H), 2.24–2.1 (m, 2H). ^{13}C NMR (CDCl_3 , 75 MHz): δ 144.1, 139.0, 137.6, 136.2, 130.0, 128.6, 128.5, 128.4, 128.3, 127.1, 127, 126.7, 67.0, 58.6, 57.4, 38.4, 21.6. ESI-MS (m/z): 408.21 ($\text{M} + \text{Na}$). The NMR spectra for the isolated ring-opened products **12-C** and **12-T** (18 mg combined, 18% yield) were identical to those reported previously.²⁰

Computational Methods. Density functional calculations were performed using the B3LYP functional in Gaussian 03.³³

CASSCF Calculations. CASSCF calculations were carried out using GAMESS (ver. 12 Jan 2009 R1).³⁴ The full Newton–Raphson (FULLNR) orbital update algorithm is used. For single-point CASSCF energy calculations, the geometries were optimized using Gaussian 03 with the B3LYP functional. A mixed basis set of LANL2DZ for Cu and 6-31G(d) for other atoms is used in the geometry optimization.

KIE Calculations. Kinetic isotope effect calculations were done using Gaussian 03. The B3LYP functional and a mixed basis set of LANL2DZ for Cu and 6-31G(d) for other atoms was used. A scaling factor of 0.9613 was used to correct the calculated frequencies.³⁵ The kinetic isotope effects on the C–H insertion transition states *singlet*- and *triplet*-**TS14** were calculated, and the results are shown in Table S1. The $k_{\text{H}}/k_{\text{D}}$ are calculated from the differences of the Gibbs free energies of the H/D-substituted transition states at 298 K. KIEs with tunneling corrections ($k_{\text{H}}/k_{\text{D}}(\text{W})$) were calculated using Wigner’s tunneling correction.³⁶ These calculations suggest that the tunneling effects in both singlet and triplet transition states are small (+20%). The calculated KIEs without tunneling corrections were used in this article.

Acknowledgment. We thank Prof. Karl Trindle (U. Virginia), who aided in the initial phase of the computational studies begun by K.N. during a sabbatical leave at UCLA. K.N. and D.B. are grateful for financial support provided by the National Science Foundation (CHE-0848591). P.L. and K.N.H. also thank the National Science Foundation for financial support (CHE-0548209). Calculations were performed on the National Science Foundation Terascale Computing System at the NCSA and the UCLA ATS and IDRE clusters.

Supporting Information Available: Spectroscopic data for all new compounds, optimized geometries and energies, diagrams of orbitals in the active space for *singlet*- and *triplet*-**13** and *singlet*- and *triplet*-**TS14**, details of IRC calculations on the *singlet*- and *triplet*-**TS14**, singlet/triplet splitting calculations with a full ligand, and complete ref³³. This material is available free of charge via the Internet at <http://pubs.acs.org>.

(33) Frisch, M. J.; et al. *Gaussian 03*, Rev. D.01; Gaussian, Inc.: Wallingford, CT, 2004.

(34) Schmidt, M. W.; Baldridge, K. K.; Boatz, J. A.; Elbert, S. T.; Gordon, M. S.; Jensen, J. H.; Koseki, S.; Matsunaga, N.; Nguyen, K. A.; Su, S. J.; Windus, T. L.; Dupuis, M.; Montgomery, J. A. *J. Comput. Chem.* **1993**, *14*, 1347.

(35) Wong, M. W. *Chem. Phys. Lett.* **1996**, *256*, 391.

(36) Wigner, E. P. *Z. Phys. Chem.* **1932**, *B19*, 203.